# Structural relaxation of adlayers in the presence of adsorbate-induced reconstruction: $C_{60}$/Cu(111)

Woei Wu Pai,[1,*] Ching-Ling Hsu,[1,†] M. C. Lin,[2] K. C. Lin,[2] and T. B. Tang[3]
[1]*Center for Condensed Matter Sciences, National Taiwan University, Taipei, Taiwan, Republic of China*
[2]*Department of Physics, Fu Jen Catholic University, Taipei, Taiwan, Republic of China*
[3]*Department of Physics, Hong Kong Baptist University, Hong Kong*
(Received 15 September 2003; revised manuscript received 18 November 2003; published 15 March 2004)

We revisit submonolayer growth of $C_{60}$ on Cu(111) by scanning tunneling microscopy (STM), with emphasis on the formation of higher-order commensurate metastable states. These phases show concomitant interfacial reconstruction, adlayer buckling, and adlayer rotation in order to match as closely as possible the 10.0 Å $C_{60}$ nearest neighbor (NN) distance. Most interestingly, a clear correlation between the adlayer rotation angle and molecular contrast patterns is demonstrated. This is caused by the $C_{60}$-induced reconstruction at preferred binding sites and adlayer buckling in adjustment to strain. Four contrast patterns, i.e., ''disordered maze,'' ''linear-wall maze,'' "$p(\sqrt{7}\times\sqrt{7})$," and "$p(2\times2)$," with increasing $C_{60}$ NN distances are categorized. In the most compressed phase, buckling is favored and it is analogous to the ground state of a strongly-coupled antiferromagnetic system on a triangular lattice with alike adlayer buckling and interfacial corrugation. In contrast, the molecular orderings in the other structures are mostly dictated by lateral displacements of $C_{60}$ toward preferred reconstructive binding sites. These metastable phases thus illustrate structural relaxation of a molecular layer on an adsorbate-induced reconstructed substrate in different adsorbate-adsorbate and adsorbate-substrate interaction limits.

DOI: 10.1103/PhysRevB.69.125405 PACS number(s): 68.43.Fg, 68.37.Ef, 64.60.My

## I. INTRODUCTION

In surface sciences one has been constantly reminded that surfaces are not rigid checkerboards on which adsorbates reside.[1] Many systems do exhibit adsorbate-induced substrate reconstruction, manifesting the subtle effects of modifying the structures of the adsorbate layers and the substrates as a whole.[2] Beyond simple adsorbate layers, adsorption of complex larger molecules is gaining more attention.[3–9] Complexities arise therein from the expanded possibilities of multiple adsorption structures, greater internal degrees of freedom, and the apparent ease of adsorbate-induced substrate reconstruction. For example, $C_{60}$ molecules have been observed to reconstruct many metal surfaces, e.g., Ni(110),[10] Au(110),[11,12] Pd(110),[13,14] Ag(100),[15,16] and Al(111).[17–20] It seems that the state of substrate reconstruction is not simply determined by the adsorbate-substrate interactions. Recent studies of $C_{60}$/Ag(100) illustrate this;[15,16,21] the $C_{60}$ adlayer does not fully reconstruct the surface and the equilibrium structure exhibits a peculiar bright-dim $C_{60}$ contrast pattern reflecting the corrugation of the $C_{60}$-substrate interface. $C_{60}$/Al(111) is another example in which a "$(\sqrt{3}\times\sqrt{3})R30°$" superstructure of $C_{60}$ contrast was reported.[17,18] It is likely that in these cases stronger adsorbate-adsorbate interactions compete with the energy gains of the adsorbate-induced reconstructions. Admittedly, the competition between adsorbate-adsorbate and adsorbate-substrate interactions is an issue that has been addressed repeatedly in experiments and theories. These include many experimental studies of inert gas adsorption on the graphite surface[22,23] and the Frenkel-Kontorova (FK) modeling of commensurate-incommensurate phase transitions.[24] Less discussed, however, is the competition of these interactions in the presence of adsorbate-induced reconstruction. We are aware of only a few FK model studies incorporating reconstructive growth.[25,26] Here we present a system, i.e., metastable state growth of $C_{60}$ on Cu(111), that illustrates the issue of structural relaxation of a molecular layer during reconstructive growth.

$C_{60}$ growth on Cu(111) is an experimental system considered well studied.[27–32] Nonetheless, the existing data set addresses only the well-ordered $p(4\times4)$ phase prepared at higher temperatures or through sufficient post-growth annealing. Grown structures at lower temperatures were often referred as disordered, implicating kinetic hindrance.[33] Signs of substrate mass transport were reported through reordering of step orientations,[28] but the impact of the mass flow on the $C_{60}$ layer structure *per se* was not elaborated. It had also been reported by photoemission that $C_{60}$ interacts more strongly with Cu(111) than with Au(111).[31] Yet, $C_{60}$ on Au(111) was shown to lift the herringbone reconstruction.[34] In light of these previous findings, we revisit the subject of $C_{60}$ growth on Cu(111), with emphasis on preparing metastable structures at lower temperatures. Our goal is twofold. First, it is expected that the influence of substrate mass flow on the $C_{60}$ adlayer structure and possible adsorbate-induced reconstruction can be monitored in these metastable phases. Second, we wish to examine the channels through which the adlayer relaxes during reconstructive growth. We find several metastable phases in which concomitant interfacial reconstruction, adlayer buckling, and adlayer rotation occur. These are all higher-order commensurate structures in which the $C_{60}$ NN distance self-adjusts to approach the ideal 10.0 Å bulk value. Four STM patterns, namely, ''disordered maze,'' ''linear-wall maze,'' "$p(\sqrt{7}\times\sqrt{7})$," and "$p(2\times2)$" phases, reveal a well-defined correlation between the adlayer rotation

 ©2004 The American Physical Society

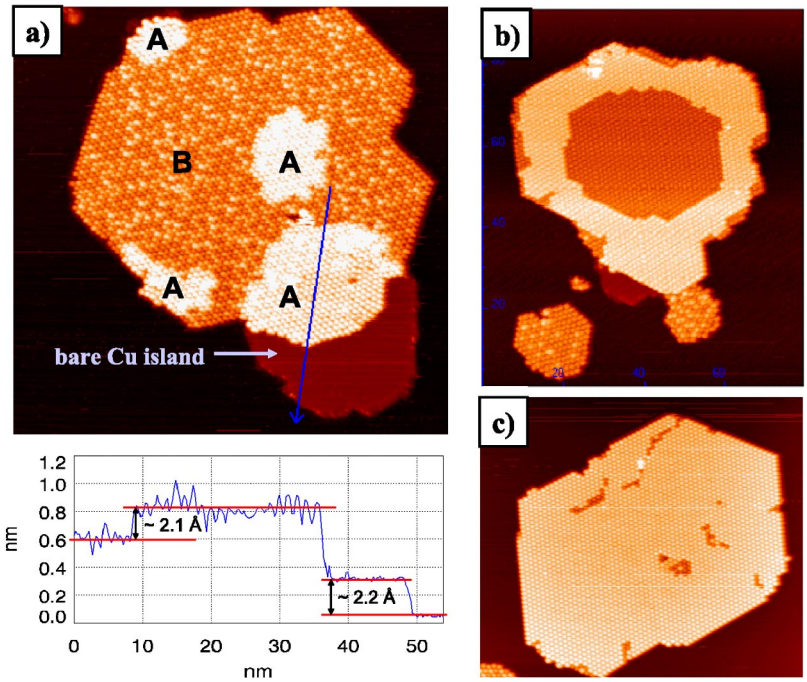


FIG. 1. (Color online) (a) A $C_{60}$ island with higher $C_{60}$ regions (A), a lower $C_{60}$ region (B), and an adjacent bare Cu island. An inset line profile passing the B, A regions, and the bare Cu island indicates a height difference between the A and B regions close to that of a Cu(111) step. Image size $98\times98$ nm$^2$; sample bias $V_s=-1.2$ V; tunneling current $I_t=0.34$ nA. (b) A "core-shell" $C_{60}$ island prepared with a two-stage deposition method as described in the text. Image size $80\times94$ nm$^2$; $V_s=-1.1$ V; $I_t=0.93$ nA. (c) A "$p(4\times4)$-LT" island prepared at room temperature. Image size $85\times75$ nm$^2$; $V_s=-1.5$ V; $I_t=0.97$ nA.

angle and the $C_{60}$ contrast ordering. This contrast ordering can be understood in light of different relative strengths of adsorbate-adsorbate (AA) and adsorbate-(reconstructed) substrate (AS) interactions. This is illustrated by a heuristic employment of an antiferromagnetic like AA interaction and an optimization of the AS interaction in the unit cell of each metastable phase.

## II. EXPERIMENT

Experiments were conducted with a variable temperature multimode scanning probe microscope (Omicron VTSPM) housed in a homebuilt ultrahigh-vacuum chamber ($P_{base}\sim4\times10^{-11}$ torr) described previously.[15] The Cu(111) crystal was cleaned by repeated sputter-anneal ($\sim850$ K) cycles with neon. Submonolayer of $C_{60}$ (>99.95% purity) was deposited from an electron-beam evaporator with a thoroughly outgased Ta crucible in a preparation chamber. STM imaging was performed separately in the VTSPM chamber. During $C_{60}$ growth, a nominal substrate temperature of 250–550 K and a deposition rate of $\sim0.03$ ML/min (1 ML=1 monolayer of fully covered $C_{60}$) were used. The pressure was below $10^{-10}$ torr during the deposition. Metastable structures were prepared at lower dosing rates to avoid kinetically hindered disordered structures. The sample temperature was calibrated against a thermocouple on the manipulator head, and on the STM stage by a Si diode mounted on a cooling block in direct thermal contact with the Cu crystal.

## III. RESULTS AND DISCUSSION

### A. $C_{60}$-induced substrate reconstruction and structure of the ordered $p(4\times4)$ phase

Before elaborating on the metastable $C_{60}$ structures, we present two new findings, i.e., evidence of adsorbate-induced reconstruction and the lack of multiplicity in adsorption sites of the $p(4\times4)$ ordered phase. The former is deduced from a direct observation of substrate mass flow associated with the $C_{60}$ layer and a distinct "core-shell" island structure prepared with a two-step growth method.[15,16] The latter, as derived through an analysis of the relative displacement of adjacent $C_{60}$ domains, shows that there is only one type of favored adsorption site in the $p(4\times4)$ phase. This is in contrast to the previous reports claiming the $p(4\times4)$ structure may occupy either the fcc or hcp sites.[27,28] As will be discussed in Sec. III B, both findings are important for understanding the structures of the metastable states.

The STM evidence of possible adsorbate-induced reconstruction could come from monitoring structural evolution during adlayer formation. For example, monitoring the step motion during oxygen adsorption on Ag(110) validates the so-called "added row" structure.[35] Similarly, we examined the formation of $C_{60}$ layers at lower temperatures, i.e., <370 K, in search of signs of substrate mass flow. A lower temperature was used to limit Cu adatom diffusion to nearby steps and the signature of $C_{60}$-induced reconstruction was expected to occur on wider terraces. Indeed, nucleated bare Cu regions nearby $C_{60}$ islands were often observed. This is shown in Fig. 1(a). In fact, many $C_{60}$ islands were overgrown on top of such nucleated Cu islands, forming a "double-layer" structure. In Fig. 1(a), patches of $C_{60}$ regions (denoted by A) appear higher than the rest (denoted by B). A line profile passing the B, A regions, and the bare Cu island is shown in Fig. 1(a) (inset). It is clear that the height difference between the A and B regions is close to that of a Cu(111) single-height step, $\sim2.08$ Å. This height is certainly too small for the diameter of a $C_{60}$ molecule. The A region is therefore not an additional $C_{60}$ layer on top of the B region; it must be interpreted as a single-layer $C_{60}$ island with a nucleated Cu island underneath. Note that we never observed

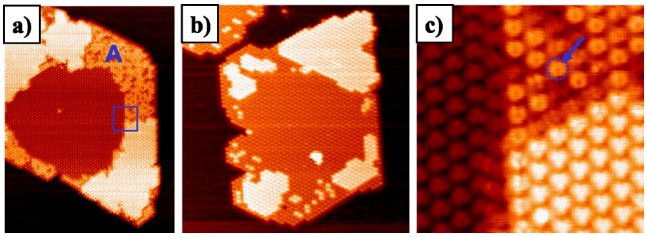


FIG. 2. (Color online) (a), (b) Temperature evolution of a core-shell island. (a) Upon annealing at ~340 K for ~250 s, the shell develops regions of lower heights (e.g., the A region). Image size $65\times85$ nm$^2$; $V_s=-0.67$ V; $I_t=1.43$ nA. (b) Further annealing at ~380 K causes a significant portion of the shell area to transform to the core $C_{60}$. Image size $60\times60$ nm$^2$; $V_s=-1.1$ V; $I_t=0.93$ nA. (c) A magnified view of the boxed region in (a) reveals an orientation change of $C_{60}$ (denoted by an arrow) from that of the core and shell $C_{60}$ showing threefold lobes. Image size $10\times10$ nm$^2$; $V_s=-0.67$ V; $I_t=1.43$ nA.

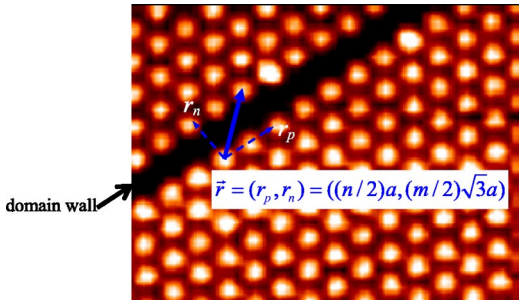


FIG. 3. (Color online) An STM image of a $p(4\times4)$ region with a domain boundary. The offset vector $\vec{r}=(r_p,r_n)$ is labeled; $m$, $n$ are integers and $a$ is the NN Cu distance. Image size: $14\times10$ nm$^2$; $V_s=0.6$ V; $I_t=0.75$ nA.

bare Cu islands on the clean pristine Cu substrate at room temperature or the $C_{60}$ growth temperatures. We also note that the ''double-layer'' $C_{60}$ islands were quite common as long as the growth temperature was suitably chosen, and they tended to form at regions away from steps. These observations convinced us that $C_{60}$ induced a Cu substrate mass flow originated from the substrate terraces, i.e., $C_{60}$-induced substrate reconstruction must have occurred. Similar ''double-layer'' $C_{60}$ islands have both been observed for $C_{60}/Ag(100)$[16] and $C_{60}/Cu(100)$.[36] Substrate reconstructions were inferred therein in both cases.

The ordered $p(4\times4)$ structure also has a reconstructed interface. Although it was typically prepared at higher temperatures and hence the ''double-layer'' $C_{60}$ structure or bare Cu islands were less frequently observed, the $C_{60}$-induced reconstruction can also be revealed from another perspective. If one prepared first the ordered $p(4\times4)$ islands at higher temperatures followed by subsequent $C_{60}$ deposition at room temperature or below, distinct ''core-shell'' islands formed.[15] The $p(4\times4)$ ordering was observed in both the ''core'' and ''shell'' regions, but the STM $C_{60}$ heights differed by ~2.2 Å. Such a height difference was much larger than the surface corrugation of Cu(111) and was unlikely due to a mere height variation at different adsorption sites. The height was also much smaller than the diameter of a $C_{60}$ and was therefore not due to the adsorption of a second layer $C_{60}$. *In situ* contact-mode AFM measurements (not shown) also showed that the core-shell height difference was a topographic feature. A typical core-shell island is shown in Fig. 1(b) and its temperature evolution is reported in Figs. 2(a)–2(c). Upon annealing a core-shell island to ~340 K for ~250 s, the $C_{60}$ shell developed regions of lower heights [denoted as A in Fig. 2(a)] and individual dark $C_{60}$ appeared. With further annealing at ~380 K [Fig. 2(b)], a significant portion of the shell $C_{60}$ became identical to the core region and small patches of bright $C_{60}$ remained. If a core-shell island was further annealed, all bright $C_{60}$ in the shell eventually transformed to the core $C_{60}$, i.e., the ordered $p(4\times4)$ phase. Compared with the adlayer rotation in metastable states reported below in Sec. III B, the evolution of the shell regions is different and is greatly influenced by the reconstructed core region. First, no adlayer rotation was observed. In spite of the contrast change, the shell region preserved its $p(4\times4)$ orientation. Second, no distinct and well-defined contrast pattern occurred. Finally, the orientation of an individual $C_{60}$ changed as its contrast varied. Figure 2(c) shows a magnified view of the boxed region of Fig. 2(a). In the upper-right $C_{60}$ region of a lower height, the $C_{60}$ orientation (denoted by an arrow) was different from that of the core and shell $C_{60}$ showing threefold lobes.[27] This $C_{60}$ orientation change was understood as a direct consequence of the substrate reconstruction.

Both the substrate mass flow and the change of the $C_{60}$ contrast upon thermal activation can be rationally interpreted as results from the $C_{60}$-induced substrate reconstruction. Previously, reordering of Cu(111) steps toward the close-packed directions after $C_{60}$ growth was interpreted as a sign of substrate mass flow.[28] Our results strengthen these prior findings.

While detailed information on the interfacial structure is difficult to obtain with STM, the observed long range mass transport indicates that the reconstruction should not be simply a local rearrangement of Cu atoms. Instead, a vacancy or vacancies underneath $C_{60}$ should be likely.[12,16,20] Furthermore, one can infer whether there are multiple $C_{60}$ adsorption sites in the $p(4\times4)$ structure. This is made possible by examining the relative $C_{60}$ positions across adjacent $p(4\times4)$ domain boundaries. Sakurai *et al.* reported such an analysis[27,28] and concluded that the $p(4\times4)$ phase can occupy either the fcc or hcp sites. This conclusion was reached by analyzing the relative $C_{60}$ positions across and normal to the domain boundary, for which they found an offset of $\pm1/3a$ ($a$: the nearest neighbor Cu distance $a=2.56$ Å). However, we obtained contradictory results based on analyzing the relative $C_{60}$ positions normal *and* parallel to the domain boundaries. It shows that only one type of adsorption site exists. This can be either the fcc or hcp sites. Figure 3 shows an STM image of two $p(4\times4)$ regions separated by a domain boundary. From analyzing the offset vectors, as denoted by $\vec{r}$, of 10 micrographs for $C_{60}$ films grown from 370 K to 570 K, we found that $\vec{r}$ can all be represented as $\vec{r}=(r_p,r_n)=(n(a/2),m(\sqrt{3}a/2))$, where $m$, $n$ are integers. If both the hcp and fcc $p(4\times4)$ domains exist, $\vec{r}$ should also

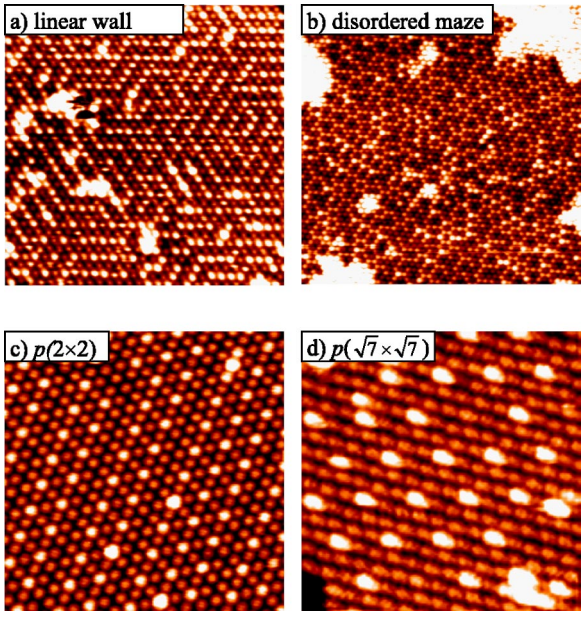


FIG. 4. (Color online) Images of the four metastable $C_{60}$ phases showing the distinct characteristic molecular contrast patterns. (a) Stage 1a—"linear-wall maze" structure. Image size: $38\times38$ nm$^2$. (b) Stage 1b—"disordered maze" structure. Image size: $59\times59$ nm$^2$. (c) Stage 2a—"$p(2\times2)$" structure. Note there are domain boundaries. Image size: $24\times24$ nm$^2$. (d) Stage 2b—"$p(\sqrt{7}\times\sqrt{7})$" structure. Image size: $19\times19$ nm$^2$.

have been expressible as $(n'(a/2),(m'+2/3)(\sqrt{3}a/2))$. Our data set is consistently closer to the former expression of $\vec{r}$.

A single preferred adsorption site for reconstructive growth has an important implication for the evolution of metastable structures as it characterizes the energy landscape of adsorbate-substrate interaction. To seek a single kind of preferred sites, larger displacements of $C_{60}$ positions are needed as compared to that of multiple preferred adsorption sites. Therefore, significant changes in the $C_{60}$-$C_{60}$ interaction may arise to compete with the adsorbate-induced reconstruction. This will be particularly evident in a compressed $C_{60}$ phase as discussed below.

### B. Characterization of metastable structures of $C_{60}$ on Cu(111)

Deposition of $C_{60}$ films at lower temperatures ($\sim$280–340 K) reveals a series of metastable structures that are characterized by their rotation angles and distinct $C_{60}$ contrast patterns. Figures 4(a)–4(d) show four accessible metastable states [called stages 1a, 1b, 2a, and 2b for Figs. 4(a)–4(d), respectively]. Based on their distinct molecular contrast patterns, we coin stages 1a, 1b, 2a, 2b as (1a) "linear-wall maze," (1b) "disordered maze," (2a) "$p(2\times2)$," and (2b) "$p(\sqrt{7}\times\sqrt{7})$." Upon annealing, the 1a and 1b phases often started to appear together at $\sim$300–310 K whereas the 2a, 2b phases appeared gradually at slightly higher temperature $\sim$310–330 K. At a higher substrate temperature, e.g., 370 K, metastable structures gradually disappeared and the $p(4\times4)$ structure formed, with increased ordering by annealing. At a deposition temperature of $\sim$300 K or slightly below, patches of apparent $p(4\times4)$ ordering can be seen as well. These $p(4\times4)$ regions were actually identical to the shell regions without the $C_{60}$-induced reconstruction underneath, as shown in Fig. 1(b). This is also a metastable structure and will be termed "$p(4\times4)$-LT" to differentiate from the annealed $p(4\times4)$. Figure 1(c) gives an example of a "$p(4\times4)$-LT" island prepared at room temperature.

Since the apparent adsorption registries of the $p(4\times4)$-LT and $p(4\times4)$ structures are identical except for their interfacial structures, occurrence of the four metastable states (stages 1a–2b) must be related to the onset of the $C_{60}$-induced reconstruction. Conceptually, this is because the $C_{60}$-induced substrate reconstruction alters the relative strengths of the competing $C_{60}$-$C_{60}$ and $C_{60}$-Cu interactions. Experimentally, the resulting phenomena are complicated, involving several concomitant competing forces. These are (a) adlayer rotation for an optimal coincidence lattice matching, (b) optimal coordinations of $C_{60}$ at preferred reconstructive binding sites, and (c) variation of the $C_{60}$-$C_{60}$ interaction due to lattice distortion. We demonstrate that the four metastable phases can be understood with these competing forces in different limits.

We tabulate structural parameters of the metastable phases in Table I, and use the $p(2\times2)$ phase as an example to

TABLE I. Structural parameters of all the $C_{60}$ phases observed on Cu(111).

| Stage | Rotation angle($\theta$) (observed) | Rotation angle($\theta$) (predicted) | Contrast pattern | $C_{60}$ STM height | Dim $C_{60}$ ratio(%)[a] | Coincidence lattice | In-plane $C_{60}$-$C_{60}$ $r$ (Å) |
|---|---|---|---|---|---|---|---|
| | 30° | 30° | $p(4\times4)$-LT | I | $\sim$0 | $1\times1$ | 10.224 |
| 1a | $\pm3$–4° | $\pm3.67°$ | linear-wall maze | II, III, V | $\sim$50 | $2\times2$ | 9.982 |
| 1b | $\pm6$–8° | $\pm7.59°$ | disordered maze | I, III, V | $\sim$50 | $\sqrt{3}\times\sqrt{3}$ | 9.654 |
| 2a | $\pm11$–12° | $\pm10.89°$ | $p(2\times2)$ | III, V | $\sim$75 | $2\times2$ | 10.144 |
| 2b | $\pm19$–20° | $\pm19.11°$ | $p(\sqrt{7}\times\sqrt{7})$ | IV, V | $\sim$85 | $\sqrt{7}\times\sqrt{7}$ | 10.040 |
| | 30° | 30° | $p(4\times4)$ | V | $\sim$100 | $1\times1$ | 10.224 |

[a]Dim $C_{60}$ are those with the lowest observed STM height in each phase.

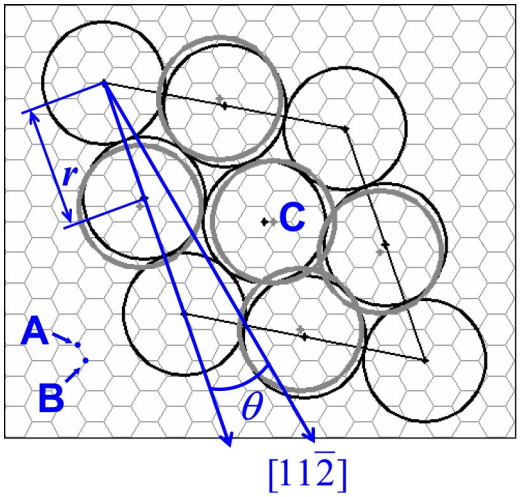


FIG. 5. (Color online) A schematic drawing of the $p(2\times2)$ phase with notations of Table I. The rhombic $p(2\times2)$ unit cell is shown. Black circles denote $C_{60}$ at undistorted positions. Gray circles are the "dim" $C_{60}$ molecules fully distorted to the nearest reconstructive binding sites. The underlying honeycomb lattice consists of all hollow sites of a fcc(111) surface. A and B label the occupied sites for the apex and nonapex $C_{60}$ in the distorted $C_{60}$ lattice, respectively. C denotes the middle $C_{60}$ in the unit cell.

illustrate definitions of notations, as depicted in Fig. 5. The orientation of the $C_{60}$ lattice is denoted by a rotation angle $\theta$ measured counter clockwise from $\langle 11\bar{2}\rangle$. This $\theta=0$ direction and the surface normal define a mirror plane. Phases of $\theta$ and $-\theta$ are therefore structurally equivalent and they are indeed both observed. The coincidence lattice specifies the unit cell, e.g., $(2\times2)$, of the $C_{60}$ lattice that defines the new commensurate periodicity with the Cu substrate. Note that the apex $C_{60}$ of the coincidence lattice occupy a single type of site (labeled as site A in Fig. 5) but we do not specify whether it is the hcp or fcc sites.[37] Finally, $r$ represents the NN $C_{60}$-$C_{60}$ distance. The $p(2\times2)$ phase thus is denoted as $(2\times2)R(\theta\approx11°)\text{at}(r\approx10.144\ \text{Å})$. It is clear from Table I that the coincidence lattices exist for all four metastable phases and a perfect correspondence between the measured and predicted adlayer rotation angles is apparent. The $C_{60}$-$C_{60}$ NN distance self-adjusts to the ideal bulk $C_{60}$-$C_{60}$ distance of 10.0 Å as closely as possible. This is verified by tabulating all possible configurations for each coincidence lattice occupying identical adsorption sites (not shown). The existence of the coincidence lattices shows the metastable states are higher-order commensurate phases encompassing all smaller unit cells, i.e., $(\sqrt{3}\times\sqrt{3})$, $(2\times2)$, and $(\sqrt{7}\times\sqrt{7})$. It is also noted from Table I that the dim $C_{60}$ concentration increases from the $p(4\times4)$-LT to the $p(4\times4)$ upon annealing. This corroborates well with a thermally activated scenario of the $C_{60}$-induced reconstruction. In fact, five groups of distinct $C_{60}$ STM heights, i.e., (I) 7.4 Å, (II) 7.0 Å, (III) 6.1–6.6 Å, (IV) 5.7 Å, and (V) 5.2 Å, relative to the neighboring bare Cu terraces are observed. Consequently, several interfacial structures seem to coexist. Our present STM data cannot yet underpin further details of such interfacial structures.

### C. Physical origin of $C_{60}$ contrast formation in metastable states

We can now readily discuss the tantalizing correlation between the adlayer rotation and the molecular contrast pattern. As mentioned earlier, structural relaxation of the $C_{60}$ adlayer in the presence of adsorbate-induced reconstruction is determined by three competing interactions, i.e., (a) $C_{60}$ and Cu lattice matching, (b) the $C_{60}$-induced reconstruction, and (c) the $C_{60}$-$C_{60}$ interaction. The former two terms are adsorbate-substrate interactions and the last is an adsorbate-adsorbate interaction. Uptake of the adlayer rotation arises from optimizing the $C_{60}$-$C_{60}$ interaction as the NN distance reduces to nearly 10.0 Å. Lattice matching of the Cu(111) and $C_{60}$ lattice controls the adlayer rotation angle. The final $p(4\times4)$ structure is stabilized by the $C_{60}$-induced reconstruction as the NN $C_{60}$ distance is reverted to an expanded 10.224 Å.

The characteristic $C_{60}$ contrast pattern in each mestastable phase is determined by which competing interactions are strong. The phases 2a and 2b represent the limit of weak adsorbate-adsorbate interactions. The $C_{60}$ lattices are expanded with NN distances larger than 10.0 Å. Consider again the $p(2\times2)$ phase of Fig. 5, the apex $C_{60}$ of the coincidence lattice unit cell are on an identical kind of adsorption site whereas all the other nonapex $C_{60}$ are situated on non-high-symmetry positions (as determined by the distance $r$ in Table I). These unfavorably adsorbed $C_{60}$ then displace toward preferred binding sites where the substrate reconstruction can be induced, i.e., another type of hollow site different from that of the apex $C_{60}$. It turns out that such distortion only leads to minor increase in the $C_{60}$-$C_{60}$ interaction, and all molecules reconstruct the substrate underneath except for the apex $C_{60}$ where the induced reconstruction may not develop fully. Consequently, the contrast pattern essentially mimics the $p(2x2)$ coincidence lattice. The same scenario is valid for the $p(\sqrt{7}\times\sqrt{7})$ phase.

The disordered-maze phase (1b) is highly compressed with a NN $C_{60}$ distance of only 9.654 Å. It represents a limiting case where the adsorbate-adsorbate interaction is dominating. Although the $C_{60}$ still tend to displace laterally, a fast rise of the $C_{60}$-$C_{60}$ repulsion is evident. In response to such a strong repulsion, the nearest neighbor $C_{60}$ buckle. For example, with an in-plane NN distance 9.654 Å and an out-of-plane buckling of 2.2 Å (i.e., the height difference of the bright and dim $C_{60}$), the $C_{60}$ NN distance becomes 9.90 Å. To take the advantage of the energy gain of substrate reconstruction, the interface replicates the resulting buckling pattern. The out-of-plane buckling is hence inward, rather than outward, with the substrate Cu atoms removed. Note that the NN buckling is analogous to a NN antiferromagnetic (AF)-like coupling with the upward and downward buckles similar to the up spins and down spins. On a triangular lattice, it is well known that the AF coupling results in frustrated ground states.[38] In Fig. 6, a Monte Carlo simulation snapshot of an AF ground state with a Hamiltonian $H=J\Sigma_{\langle i,j\rangle}n_in_j$, with $J\gg k_BT>0$, $\langle i,j\rangle$ for the NN pairs, and $n_i$, $n_j=\pm1$, is shown to reproduce the observed disordered-maze pattern well[39] [cf. Fig. 4(b)]. Additionally, the measured dim $C_{60}$ concentration is indeed close to 50%, as expected for the up

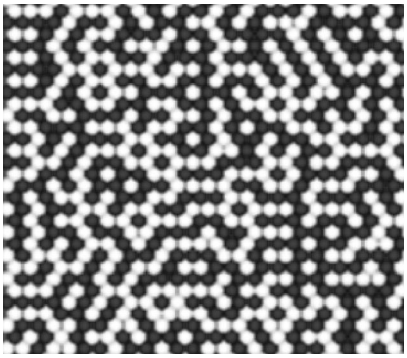

FIG. 6. A Monte Carlo simulation snapshot of a disordered-maze-like ground state with an antiferromagnetic NN coupling on a triangular lattice.

or down spins in an AF ground state with no external field. Although the disordered-maze phase has an underlying $\sqrt{3}\times\sqrt{3}$ coincidence lattice, the lack of a $\sqrt{3}\times\sqrt{3}$ contrast pattern indeed reflects that the adlayer buckling is dictated by a strong $C_{60}$-$C_{60}$ repulsion.

Finally, the linear-wall-maze phase (1a) is an intermediate case where neither the adsorbate-adsorbate nor the adsorbate-substrate interaction is dominating. Although it also has a $p(2\times2)$ coincidence lattice, its $C_{60}$ NN distance is slightly smaller as compared with that of the $p(2\times2)$ phase, implying an increased role of the $C_{60}$-$C_{60}$ repulsion. This in turn modifies the contrast pattern in a way that the middle $C_{60}$ (labeled as C in Fig. 5) in the $(2\times2)$ unit cell remains ''bright,'' leaving the substrate underneath unreconstructed. The unit cell depicted in Fig. 5 can then be translated and rotated with proper symmetry operations, leading to the observed linear-wall-maze pattern. To augment the above heuristic arguments, we calculate the increase in the $C_{60}$-$C_{60}$ interaction energy using the Girifalco potential[40] in both the unit cells of phases 1a and 2a, assuming all the nonapex $C_{60}$ fully displacing to the closest preferred reconstructive binding sites (i.e., B-type sites in Fig. 5). We find that in the $p(2\times2)$ phase and the linear-wall-maze phase the $C_{60}$-$C_{60}$ interaction increases by 2.27 eV per $C_{60}$ and 15.00 eV per $C_{60}$, respectively. If in the linear-wall-maze phase the inward buckle and in-plane displacement of the middle $C_{60}$ are inhibited, the energy cost reduces to 5.26 eV per $C_{60}$. Such a large difference of $\sim$9.74 eV per $C_{60}$ presumably explains why the middle bright $C_{60}$ would not reconstruct the substrate.

In summary, monolayers of $C_{60}$ grown on Cu(111) result in substrate reconstructions that strongly affect the adlayer structural relaxation. Several metastable states are characterized and a clear correlation of the adlayer rotation and characteristic $C_{60}$ contrast patterns is explained. This is due to a delicate balance between the competing $C_{60}$-Cu and $C_{60}$-$C_{60}$ interactions. Our system manifests an interesting chemisorption case in which the relative strengths of adsorbate-adsorbate and adsorbate-substrate interactions are ''tuned'' through adsorbate-induced reconstructions. Similar behaviors can be expected for systems where molecular films reconstruct their substrates.

## ACKNOWLEDGMENTS

We acknowledge technical assistance by Dr. Y. L. Chan, L. Y. Sin, and C. J. Yiu. This work is supported by Grant Nos. NSC90-2112-M-002-034 and NSC-91-2112-M-002-038, Taiwan, R.O.C, and Grant No. RGC-32-02-050, Hong Kong S.A.R.

*Corresponding author. Electronic address: wpai@ccms.ntu.edu.tw
†Current address: Department of Physics, Chung Yuan Christian University, Chung-Li, Taiwan, R.O.C.

[1] D. P. Woodruff, Surf. Sci. **500**, 147 (2002).
[2] S. Titmuss, A. Wander, and D. A. King, Chem. Rev. (Washington, D.C.) **96**, 1291 (1996).
[3] T. A. Jung, R. R. Schlittler, J. K. Gimzewski, H. Tang, and C. Joachim, Science **271**, 181 (1996).
[4] G. E. Poirier, Chem. Rev. (Washington, D.C.) **97**, 1117 (1997).
[5] F. Rosei, M. Schunack, Y. Naitoh, P. Jiang, A. Gourdon, E. Laegsgaard, I. Stensgaard, C. Joachim, and F. Besenbacher, Prog. Surf. Sci. **71**, 95 (2003).
[6] F. Rosei, M. Schunack, P. Jiang, A. Gourdon, E. Laegsgaard, I. Stensgaard, C. Joachim, and F. Besenbacher, Science **296**, 328 (2002).
[7] F. Moresco, L. Gross, M. Alemani, K. H. Rieder, H. Tang, A. Gourdon, and C. Joachim, Phys. Rev. Lett. **91**, 036601 (2003).
[8] G. V. Nazin, X. H. Qiu, and W. Ho, Science **302**, 77 (2003).
[9] X. H. Qiu, G. V. Nazin, and W. Ho, Science **299**, 542 (2003).
[10] P. W. Murray, M. O. Pedersen, E. Laegsgaard, I. Stensgaard, and F. Besenbacher, Phys. Rev. B **55**, 9360 (1997).
[11] J. K. Gimzewski, S. Modesti, and R. R. Schlittler, Phys. Rev. Lett. **72**, 1036 (1994).
[12] M. Pedio, R. Felici, X. Torrelles, P. Rudolf, M. Capozi, J. Rius, and S. Ferrer, Phys. Rev. Lett. **85**, 1040 (2000).
[13] J. Weckesser, J. V. Barth, and K. Kern, Phys. Rev. B **64**, 161403 (2001).
[14] J. Weckesser, C. Cepek, R. Fasel, J. V. Barth, F. Baumberger, T. Greber, and K. Kern, J. Chem. Phys. **115**, 9001 (2001).
[15] W. W. Pai, C. L. Hsu, C. R. Chiang, Y. Chang, and K. C. Lin, Surf. Sci. **519**, L605 (2002).
[16] W. W. Pai and C. L. Hsu, Phys. Rev. B **68**, 121403(R) (2003); C. L. Hsu and W. W. Pai, *ibid.* **68**, 245414 (2003).
[17] A. J. Maxwell, P. A. Bruhwiler, S. Andersson, D. Arvanitis, B. Hernnas, O. Karis, D. C. Mancini, N. Martensson, S. M. Gray, M. K. J. Johansson, and L. S. O. Johansson, Phys. Rev. B **52**, R5546 (1995).
[18] M. K. J. Johansson, A. J. Maxwell, S. M. Gray, P. A. Bruhwiler, and L. S. O. Johansson, Surf. Sci. **397**, 314 (1998).
[19] A. J. Maxwell, P. A. Bruhwiler, D. Arvanitis, J. Hasselstrom, M. K. J. Johansson, and N. Martensson, Phys. Rev. B **57**, 7312 (1998).
[20] M. Stengel, A. D. Vita, and A. Baldereschi, Phys. Rev. Lett. **91**, 166101 (2003).
[21] M. Grobis, X. Lu, and M. F. Crommie, Phys. Rev. B **66**, 161408 (2002).
[22] *Ordering in two dimensions*: Proceedings of an International Conference held at Lake Geneva, Wisconsin, USA, edited by S. K. Sinha (Elsevier-North-Holland, Amsterdam, 1980).
[23] A. Thomy, X. Duval, and J. Regnier, Surf. Sci. Rep. **1**, 1 (1981).

[24] R. Pushpa and S. Narasimhan, Phys. Rev. B **67**, 205418 (2003).
[25] O. M. Braun and M. Peyrard, Phys. Rev. B **51**, 17158 (1995).
[26] O. M. Braun and M. Peyrard, Phys. Rev. E **51**, 4999 (1995).
[27] T. Hashizume, K. Motai, X. D. Wang, H. Shinohara, Y. Saito, Y. Maruyama, K. Ohno, Y. Kawazoe, Y. Nishina, H. W. Pickering, Y. Kuk, and T. Sakurai, Phys. Rev. Lett. **71**, 2959 (1993).
[28] T. Sakurai, X. D. Wang, T. Hashizume, V. Yurov, H. Shinohara, and H. W. Pickering, Appl. Surf. Sci. **87–8**, 405 (1995).
[29] Y. Maruyama, K. Ohno, and Y. Kawazoe, Phys. Rev. B **52**, 2070 (1995).
[30] A. Fartash, J. Appl. Phys. **79**, 742 (1996).
[31] K. D. Tsuei and P. D. Johnson, Solid State Commun. **101**, 337 (1997).
[32] K. D. Tsuei, J. Y. Yuh, C. T. Tzeng, R. Y. Chu, S. C. Chung, and K. L. Tsang, Phys. Rev. B **56**, 15412 (1997).
[33] T. Sakurai, X. D. Wang, Q. K. Xue, Y. Hasegawa, T. Hashizume, and H. Shinohara, Prog. Surf. Sci. **51**, 263 (1996).
[34] E. I. Altman and R. J. Colton, J. Vac. Sci. Technol. B **12**, 1906 (1994).
[35] W. W. Pai and J. E. Reutt-Robey, Phys. Rev. B **53**, 15 997 (1996).
[36] M. Abel, A. Dmitriev, R. Fasel, N. Lin, J. V. Barth, and K. Kern, Phys. Rev. B **67**, 245407 (2003).
[37] It is possible that some $C_{60}$ in the metastable states may have occupied less favorable adsorption registries, e.g., the atop site or non-high-symmetry positions. To simplify the model without sacrificing its physical essence, we limit our discussion to the (111) hollow sites.
[38] H. Kawamura, J. Phys.: Condens. Matter **10**, 4707 (1998).
[39] L. Ottaviano, B. Ressel, C. Di Teodoro, G. Profeta, S. Santucci, V. Chab, and K. C. Prince, Phys. Rev. B **67**, 045401 (2003).
[40] L. A. Girifalco, J. Phys. Chem. **95**, 5370 (1991).